NBSIR 81-2320

A Heat Transfer Analysis of Scald Injury

Center for Consumer Product Technology
National Engineering Laboratory
U.S. Department of Commerce
National Bureau of Standards
Washington, DC 20234

July 1981

Final Report

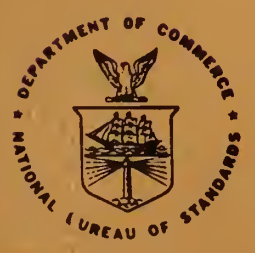

U.S. DEPARTMENT OF COMMERCE
NATIONAL BUREAU OF STANDARDS

NBSIR 81-2320

A HEAT TRANSFER ANALYSIS OF SCALD INJURY

Robert L. Palla, Jr.

Center for Consumer Product Technology
National Engineering Laboratory
U.S. Department of Commerce
National Bureau of Standards
Washington, DC 20234

July 1981

Final Report

U.S. DEPARTMENT OF COMMERCE, Malcolm Baldrige, *Secretary*
NATIONAL BUREAU OF STANDARDS, Ernest Ambler, *Director*

ABSTRACT

Numerical solutions for skin tissue temperature during scald injury events are obtained and utilized in conjunction with a thermal injury criterion, to predict critical exposure levels for various heated fluids. A one-dimensional tissue model of the type used by Love is employed to determine the initial tissue temperature distribution. The bio-heat equation for tissue heat transfer is then solved via an implicit finite difference technique, subject to convective heating and cooling at the surface.

The sensitivity of the critical exposure level to variations in tissue properties and convective heating coefficients is investigated. Thermal injury thresholds are presented for various fluids along with bounds to reflect uncertainty in assumed tissue properties. The results obtained are in good agreement with existing experimental scald injury data.

PREFACE

This report is a product of a short term research effort sponsored by the National Bureau of Standards, Center for Consumer Product Technology (CCPT). The objective of this research is a more thorough understanding of thermal injury from heated fluids -- a prerequisite for the development of improved product standards.

The work reported herein, dealing with the heat transfer aspects of thermal injury, was performed in the Product Performance Engineering Division of CCPT. Companion work in the area of thermal injury criteria was conducted concurrently in the Product Safety Division of CCPT, and provided the basis for quantifying thermal injury in the present study.

TABLE OF CONTENTS

LIST OF TABLES

LIST OF FIGURES

NOMENCLATURE

A	coefficient matrix
A	area, m^2
B	dimensionless parameter, defined by Equation 15
c_p	specific heat, J/kg K
C	thermal capacity, J/K
C	concentration of substance in blood, kg/m^3
ΔC	concentration of substance in volume element, kg/m^3
D	body part diameter, m
DA	thickness of tissue in Region A, m
DB	thickness of tissue in Region B, m
E	activation energy, cal/mol
ΔF	rate of blood flow into/out of volume element, m^3/sec
h	convective heat transfer coefficient, W/m^2 K
H	parameter h/k, m^{-1}
j	flux density of blood, $m^3/m^2 sec$
k	thermal conductivity of tissue, W/mK
κ	reaction rate constant, dimensionless
ℓ	blood flow vector
L	distance from the tissue surface to the region at which $T_t = T_a$, m
m	dimensionless parameter, defined by Equation 12
n	total number of molecules in system
n_E	number of molecules having an energy greater than E
P	number of steric events required for a reaction to occur, 3.1×10^{98}
Pr	fluid Prandtl number, dimensionless

q	metabolic heat generation rate, W/m^3
Q	quantity of substance in an organ, kg
ΔQ	quantity of substance in differential element, kg
q_o	dimensionless parameter, defined by Equation 14
R	gas constant, 2 cal/K mol
R	thermal resistance, K/W
t	time, sec
T	temperature, °C
t_1	time during heating at which T_t = 44.0 °C, sec
t_2	time during cooling at which T_t = 44.0 °C, sec
Δt	solution time step, sec
V	free stream velocity of fluid, m/sec
ΔV	volume of element, m^3
w	perfusion rate, kg/m^3 sec
W	parameter $\sqrt{w_b c_{pb}/k}$, m^{-1}
x,y,z	space coordinates in cartesian system
X	dimensionless parameter, defined by Equation 13
$\Delta X,\Delta Y,\Delta Z$	dimensions of volume element, m
Y	distance from core towards tissue surface, m
α	thermal diffusivity, m^2/sec
θ	temperature difference $T-T_a$, °C
ν	kinematic viscosity of fluid, m^2/sec
ξ	dimensionless parameter, defined by Equation 11
ρ	density, kg/m^3

ϕ	volumetric blood perfusion rate, sec^{-1}
χ	parameter $k/\rho_b c_{pb}$, m^2/sec
Ω	damage integral, 1.0 for partial thickness burn

Subscripts

a	arterial blood
(a)	pertaining to Type (a) blood vessels
A	node region nearest to tissue surface
AL	last node in Region A
b	blood
(b)	pertaining to Type (b) blood vessels
b+	surface capillaries with flow in positive x direction
b-	surface capillaries with flow in negative x direction
B	node region furthest from tissue surface
Bl	first node in Region B
BL	last node in Region B
f	fluid
n	nth node
p	due to perfusion
t	tissue at a depth of 0.01 cm
v	venous blood
x+	positive x direction
x-	negative x direction
∞	evaluated at free stream conditions

Superscripts

t	present time
t+1	future time

1. INTRODUCTION

The most common cause of thermal injury in both adults and children is scalding -- tissue damage resulting from exposure to heated fluid. Studies of the epidemiology and treatment of scald and other burn injuries are numerous in the literature; however, only a few studies attempt to define critical exposure levels, that is, the temperature of the scalding fluid and the duration of exposure just sufficient to cause thermal injury. Most notable are the studies of Moritz et al. [1] and Diack et al. [2] dealing with the establishment of a thermal injury "threshold" which defines critical exposure levels for water (see figure 1), and similar studies by Stoll [3-5], Weaver et al. [6], and Takata [7], dealing with injury from radiative heating. These quantitative studies of thermal injury are based on small samples of laboratory animals or human volunteers subjected to specific cases of thermal insult and therefore do not reflect the wide spectrum of potentially hazardous fluid exposures, including variations in fluid types and flow velocities. When used in conjunction with nervous system response times, such information can be used to establish "safe" temperature levels for fluids in the home and in industry.

The present paper explores the heat transfer aspects of the scald phenomenon as a means of extending existing experimental studies to a wide variety of fluid types and scald conditions and to exposure times shorter than those reported in the literature. The basic differential equation utilized in this study is the bio-heat equation first applied by Pennes [8] in his studies of tissue temperatures. The equation is

solved subject to convective boundary conditions via a finite difference technique, and used to determine skin tissue time-temperature histories resulting from exposure to a variety of hypothetical scald conditions. The time-temperature histories are then evaluated via a thermal injury criterion to provide a quantitative measure of predicted scald severity. Through this approach, critical exposure levels for different fluids and flows are established.

The sensitivity of the solution (thermal injury threshold) to different assumptions is also considered. These include: estimated values for the tissue properties and convective heat transfer coefficients, and the effect of the initial temperature profile. The final results are new curves defining critical exposure for fluids other than water, and bounds on the injury threshold curve for water to reflect uncertainty in the assumed properties of tissue.

2. THERMAL INJURY MODEL

2.1 Tissue Heat Transfer

Most of the existing theoretical analyses of heat transfer in living tissue have been based on the so-called bio-heat transfer equation, first applied by Pennes [8] and since used by Wissler [9-11], Chato and Shitzer [12-16], Love et al. [17], Rao et al. [18], and others. The equation is:*

$$\frac{1}{\alpha}\frac{\partial T}{\partial t} = \nabla^2 T - \frac{w_b c_{pb}}{k}(T-T_a) + \frac{q}{k} \quad . \tag{1}$$

*Symbols are defined in the Nomenclature Section.

This equation, derived in Appendix A, was obtained by establishing heat balance on a differential strip element and by assuming that blood enters the element at some fixed arterial temperature, T_a, and is brought to the temperature of the tissue, T, in the capillaries. The idealization of the thermal convective transport due to blood flow has been critically examined by several investigators [19-21]. For this analysis, the simple model is assumed to be adequate for indicating the relative importance of blood flow and other physiological phenomena.

A scald event is rather short-lived -- typically less than 5 seconds. During this time, the temperature gradient is steep near the tissue surface but diminishes rapidly with increasing tissue depth. As a result, the thickness of tissue affected is quite small with respect to the linear dimension associated with the exposed tissue surface area. A one-dimensional analysis is thus justified. Also, in view of the wide range in reported values for thermal properties of the skin and the relatively small differences from layer to layer, the skin can be considered a semi-infinite, single layer material. Using the arterial temperature as a reference point, and defining $W = \sqrt{w_b c_{pb}} / k$, the one-dimensional equation may be written:

$$\frac{1}{\alpha}\frac{\partial\theta}{\partial t} = \frac{\partial^2\theta}{\partial x^2} - W^2\theta + \frac{q}{k} \quad . \tag{2}$$

Thermal injury, which occurs with increasing severity as tissue temperature is raised beyond 44 °C, is the result of damage inflicted during each of two periods -- the heating period, when the skin is

exposed to flowing fluid, and the cooling period immediately following removal of the body part from the fluid flow. Hence, in order to account for all tissue damage, Equation 2 must be solved in two parts to obtain the complete time-temperature history.

The analytical solution for the entire scald event is quite involved. Consider, for example, the solution for the simplest case -- an initially uniform tissue temperature and sudden convective heating at the surface by a constant temperature fluid. The solution to Equation 2 without the heat generation term is:

$$\frac{\theta}{\theta_\infty} = \frac{H}{2(H^2-W^2)}\left[(H-W)\, e^{-Wx}\, \mathrm{erfc}\left(\frac{x}{2\sqrt{\alpha t}} - W\sqrt{\alpha t}\right)+(H+W)\, e^{Wx}\mathrm{erfc}\left(\frac{x}{2\sqrt{\alpha t}} + W\sqrt{\alpha t}\right)\right.$$

$$\left. - 2H\, e^{Hx+(H^2-W^2)\alpha t}\, \mathrm{erfc}\left(\frac{x}{2\sqrt{\alpha t}} + H\sqrt{\alpha t}\right)\right] \qquad (3)$$

where $H = h/k$. Note: Equation 3 is valid only for the heating portion of the scald event. An analytical solution describing the entire event -- rapid heating with a high convective coefficient, h, and gradual cooling with a low h -- is considerably more difficult to obtain, and this is even before considering an initial temperature distribution in the tissue.

To avoid the analytical complexity dictated by the scald problem, a numerical implicit finite-difference solution of Equation 2 was utilized. This solution, described in detail in Appendix B, requires

as inputs the number and spacing of temperature nodes, tissue thermal properties and fluid exposure times. Also required are convective coefficients and fluid temperatures for the initial (pre-scald), heating, and cooling periods of the scald event. Based on this information, the initial temperature as well as the complete time-temperature profile at each of the specified nodes is obtained. The result gives excellent agreement with Equation 3 for the degenerate case.

2.2 Initial Tissue Temperature Profile

The temperature of the skin tissue immediately prior to exposure to heated fluid has a pronounced effect on the outcome of the exposure -- the warmer the tissue initially, the greater the temperatures experienced throughout the heating and cooling periods, and the greater the threat of scalding. That the initial temperature is indeed important can be illustrated by considering some typical temperature levels. The core or deep body temperature is approximately 37 °C, while the surface temperature under indoor ambient conditions is about 32 °C. Hence a 5 °C differential exists from core to surface. Now, the tissue temperature at which thermal injury begins to occur is 44 °C, or 7 degrees above core temperature -- the same order of magnitude as the temperature differential in the tissue.

In the simplest case, the tissue temperature profile can be assumed flat, and assigned a value somewhere between typical surface and core or arterial temperatures -- 32 °C to 37 °C, respectively. A more

realistic approach is to consider the tissue as a slab having a fixed arterial temperature at some depth below the skin surface, and convective heat loss at the skin surface. Such an approach has been utilized successfully by Love et al. [17] in medical thermography studies and will be reviewed here.

For the boundary conditions, the origin of the system is chosen to be at a depth L below the surface of the skin such that the local temperature is equal to the arterial temperature (see figure 2). Also, the slope of the temperature at this point is equal to zero. At the surface of the skin, heat conducted to the surface is assumed equal to heat lost to ambient air via convection. Thus the boundary conditions are given as

$$T = T_a \quad \text{at} \quad Y = 0, \tag{4}$$

$$\frac{dT}{dY} = 0 \quad \text{at} \quad Y = 0, \text{ and} \tag{5}$$

$$\frac{dT}{dY} = -\frac{h}{k}(T-T_\infty) \quad \text{at} \quad Y = L\ . \tag{6}$$

Here, Y is measured from core towards surface as shown in figure 2. Rewriting the governing equation and boundary conditions in terms of dimensionless parameters results in a less cumbersome form:

$$\frac{d^2\xi}{dX^2} - m^2\xi = m^2 q_o \tag{7}$$

$$\xi = 0 \quad \text{at} \quad X = 0 \tag{8}$$

$$\frac{d\xi}{dX} = 0 \quad \text{at} \quad X = 0 \tag{9}$$

$$\frac{d\xi}{dX} = B\,[1-\xi(1)] \quad \text{at} \quad X = 1 \tag{10}$$

where the dimensionless variables, ξ, X, m, q_o, and B, are defined as follows

$$\xi = T_a - T / T_a - T_\infty \tag{11}$$

$$X = Y/L \tag{12}$$

$$m = L \sqrt{w_b c_{pb}} / k \tag{13}$$

$$q_o = q / w_b c_{pb} (T_a - T_\infty) \tag{14}$$

$$B = hL/k \ . \tag{15}$$

The solution to Equation 7 may be obtained by applying boundary conditions (8) and (10):

$$\xi(X) = q_o \cosh(mX) + \{[B - Bq_o \cosh(m) + q_o B - q_o m \sinh(m)]/$$

$$[m \cosh(m) + B \sinh(m)]\} \sinh(mX) - q_o \ . \tag{16}$$

The dimension L can be eliminated through application of boundary condition (9) to Equation 16. The result is

$$q_o = q_o \frac{m}{B} \sinh (m) + q_o \cosh (m) - 1 . \qquad (17)$$

By assigning values to the parameters q_o and $\frac{m}{B} = \sqrt{w_b c_{pb} k} / h$, the value of m is determined by iterative solution of Equation 17. Core depth L can then be obtained from Equation 13. Substituting Equation 17 into Equation 16 yields the following simplification

$$\xi(X) = q_o [\cosh (mX) - 1] . \qquad (18)$$

This expression defines the initial tissue temperature profile. Its dependence on all tissue parameters including w_b and h should be noted.

2.3 Thermal Injury Criterion

Once the time-temperature history of skin tissue is obtained from the solution of Equation 2, the extent of thermal injury can be quantified by applying an appropriate injury criterion to the history. In this way, the severity of the corresponding fluid exposure is assessed.

Several thermal injury criteria have been reported in the literature [6,7,22-25]. All of these have the same form mathematically, that is, injury is proportional to an integral of an Arrhenius rate expression; however, significant differences exist in reported values for

the empirical rate constants P and E. The criterion used in the present study is that originally proposed by Henriques [22] and recently modified by Wu [24]:

$$\Omega = P \cdot \int_{t_1}^{t_2} \exp\,[-E/RT_t]\,dt \quad . \tag{19}$$

Here, T_t represents the time-varying tissue temperature at a depth of 0.01 cm, and t_1 and t_2 denote the times at which the temperature rises above and falls below 44 °C (the temperature at which injury begins to occur).

The rationale for selecting this criterion over other criteria reported in the literature is provided in Appendix C, along with a development of the basic criterion form.

3. PARAMETER VALUES

The values assigned to the tissue and convective parameters will affect the initial tissue temperature profile as well as the thermal response of the skin during the actual scald event. Thus it is important that these values be carefully chosen.

3.1 Tissue Properties

Tissue properties were selected based on a review of the literature. Typical values and ranges of values, obtained from Refs. [3,14,17,18,26-32], are presented in Table 1. For the more easily quantified tissue properties,

such as density and specific heat, little disagreement exists between reported values. However, determination of other properties, including tissue thermal conductivity and blood perfusion, is the subject of much ongoing research and cited values differ widely.

Values for the base case were assumed to be those most frequently cited in the literature. For tissue conductivity and specific heat, values of 0.42 W/mK and 4.2×10^{-3} J/kg K were used respectively. Blood perfusion rate and specific heat were taken to be 0.4 kg/m^3sec and 3.9×10^{-3} J/kg K, while a metabolic heat generation rate of 420 W/m^3 was assumed. Because of uncertainty in the values of the latter three properties, their influence on the thermal injury threshold was investigated through a sensitivity analysis.

Tissue thermal conductivity has a range of at least two to one, as seen in Table 1. When the process of sweating comes into play, the effective thermal conductivity has a range of about four to one [31]. To determine the effect of this wide variation on the injury threshold, the base case value was increased and decreased by a factor of two. New injury thresholds corresponding to each extreme were then obtained and compared to the threshold established using the base case value.

As shown in Table 1, reported values for blood perfusion rate, w_b, vary even more substantially -- from 0.1 to 7.0 kg/m^3sec in the resting state. Variation is due to differences in body region and measurement techniques. In addition, though, vaso-dilation and constriction also affect the blood perfusion rate. Local heating can bring about vessel vaso-dilation in which the blood flow through the skin can increase

to as much as 100 times the minimum rate [31]. Similarly, large variations in metabolic heat generation rate, q, are possible. However, since oxygen supplied via blood perfusion is necessary to support the metabolic reaction, a relationship between blood perfusion and metabolic heat generation can be assumed. Following Rao et al. [18], the ratio $q/w_b c_{pb}$ was taken to be constant. The base case values for q, w_b, and c_{pb} then yield a ratio value of 0.27 -- close to the suggested value of 0.3. Keeping this ratio constant fixes the value of q for each w_b and thus eliminates the need to consider separately the sensitivity of the solution to variations in w_b and q. Instead, the effect of these parameters can be determined simultaneously. Calculations were performed for one-tenth and ten-times the base case values of w_b and q, that is, $w_b = 0.04$ kg/m^{3}sec, $q = 42$ W/m^3; and $w_b = 4.0$ kg/m^{3}sec, $q = 4200$ W/m^3.

3.2 Heat Transfer Coefficients

The convective heat transfer coefficient for the pre-scald, steady-state condition was based on the empirical relationship developed by Rao et al. [18],

$$h = [6.74 + 12.1 \sqrt{V}] \text{ W/m}^2\text{K} \qquad (20)$$

where V is the air velocity in m/sec. For natural circulation of room air, an h value of 13 W/m^{2}K was obtained.

Values for h during heating were obtained from empirical relationships reported in the heat transfer literature for a cylinder in crossflow. The convective coefficient was taken to be that at the stagnation point since this represents maximum heat flux. For stagnation point heat transfer, Squire [33] gives:

$$h = 1.14\ k/D\ (VD/\nu)^{0.5}\ (Pr)^{0.4}\ . \qquad (21)$$

Values of h for fluids which typically cause thermal injury (namely, water, oil, and air) are given in Table 2. They range from 12,500 W/m^2K for high velocity water to 13 W/m^2K for low velocity air. The greater scald potential of water is obvious due to its much higher heat transfer coefficient h. The h value for the forced convection fluid heating in the experiments of Moritz [1] was assumed, in this study, to be 12,500 W/m^2K; this value was used as the base case. Values for flowing oil and hot air were also used to show the effect of different fluids on the injury threshold.

For the cooldown portion of the scald event, a value of h representative of cooling by low velocity air and evaporation was selected. This value was 21 W/m^2K.

4. NUMERICAL SIMULATIONS

Using base case parameter values and the initial tissue temperature distribution defined by Equation 18, tissue time-temperature histories at a tissue depth of 0.01 cm are shown in figure 3. These are

for a one second exposure to 70 °C water and a five second exposure to 60.2 °C water. It can be noted that the cooling period accounts for the majority of the time spent above the 44 °C damage temperature. However, since the tissue temperatures experienced during cooling are significantly lower than during heating, damage inflicted during the cooling period only amounts to about 20 percent of the total. More details on the breakdown of tissue damage are provided in Appendix C.

Application of the thermal injury criterion, Equation 19, to a time-temperature history yields a quantitative measure of scald severity, Ω. Defining $\Omega \equiv 1$ at the onset of irreversible thermal injury, the locus of critical exposure times and corresponding critical fluid temperatures can be determined iteratively. This locus, termed the "injury threshold", is a function of the particular exposure conditions (h values) and assumed tissue properties.

The thermal injury threshold generated using base case tissue properties and convective coefficients is shown in figure 4. Excellent agreement between the predicted threshold and limited experimental results of Moritz and Henriques can be noted. The new threshold extends to exposure times as short as 0.1 second and water temperatures above 100 °C. It indicates that exposure to boiling water might be tolerated if the duration of exposure is less than 0.2 seconds. This prediction takes into account the damage inflicted during the cooling period following 0.2 seconds.

4.1 Sensitivity Analysis for Tissue Properties

The uncertainty in the predicted injury threshold of figure 4 due to errors in assumed tissue properties can be estimated by considering the previously noted ranges in properties. Increasing the tissue thermal conductivity by a factor of two results in a shift of the threshold towards more conservative exposures (for the same exposure time lower fluid temperatures are permissible). Lower fluid temperatures are permissible because with increased tissue conductivity, heat penetrates the tissue much more readily. Reductions in injurious fluid temperature of 10 °C and 5 °C are predicted for 0.1 second and 1.0 second exposures respectively as shown in figure 5. Conversely, reducing the tissue conductivity by a factor of two results in an injury threshold shift of the same magnitude but in the opposite direction.

A similar effect on the injury threshold is observed when considering the variation of blood perfusion and metabolic heat generation rates (both are varied simultaneously such that the ratio $q/w_b c_{pb}$ remains constant). Increasing the rates by a factor of ten results in a shift towards more conservative exposures while decreasing the rates by a factor of ten results in an opposite effect. The range in the threshold is shown in figure 6. The shift in the threshold depicted in figure 6 is counter to what one would expect intuitively if the blood perfusion was only thought of as a tissue cooling mechanism. The more significant effect of the blood flow and heat generation, however, is in determining the initial tissue temperature profile. With high blood perfusion and heat generation rates, higher initial tissue temperatures

will be realized and thus more conservative exposures should be predicted, as they are in figure 6.

The significance of the initial tissue temperature is illustrated in figure 7 in which the thermal injury threshold is shown for different initial temperatures. For an initially flat temperature profile at 32 °C, the threshold coincides with that for the base case. This result is expected because the initial tissue surface temperature predicted by Equation 18 for base case values is 32 °C, and because the tissue depth on which the criterion (Equation 19) is based is only 0.01 cm below the surface. The effect of an initially flat profile at 37 °C is much different, the threshold for this case being shifted towards more conservative exposures as expected. This shift is similar to the one depicted in figure 6 for high blood perfusion and heat generation rates.

The influence of the initial ambient air temperature on the injury threshold is shown in figure 8. The threshold is shifted upward and downward for lower and higher ambient air temperatures respectively. For both figues 7 and 8, shifts in the injury threshold are due purely to changes in the initial tissue temperature profile, since the tissue properties and heating and cooling convective conditions are unaltered.

The maximum possible deviation in the injury threshold would occur with simultaneous, additive-type errors in each tissue property. Although such an occurrence is unlikely, the cumulative effect can alter the threshold dramatically. The effect of a worst case combination of parameters is shown in figure 9. Here the actual threshold is bound by

an upper and a lower limit. The upper limit represents a combination of low tissue thermal conductivity, low blood perfusion and metabolic heat generation rates and low initial air temperature. Conversely, the lower limit represents a combination of high values for these parameters. Maximum errors of as much as 40 °C for exposures of 0.1 second duration are possible, diminishing to less than 5 °C for exposures lasting 5 seconds or longer. The contribution of the initial tissue temperature profile to this wide range is apparent from consideration of figure 10. Comparison of tissue surface temperatures in figure 10 reveals a difference in initial tissue temperatures of 15 °C between the upper limit and the lower limit cases. Despite the wide bound on the injury threshold shown in figure 9, for typical applications a much narrower band is expected.

4.2 Effect of Heat Transfer Coefficients

An important aspect of the injury model is that the effect of different fluid types and flow conditions can be evaluated. The injury threshold for exposures to flowing water, oil, and air are shown in figure 11 using base case tissue properties and convective heating coefficients of 13000, 2500, and 46 W/m^2K respectively. For all three fluids, base case values for the initial and cooling period convective coefficients were used -- 13 and 21 W/m^2K respectively. As shown in figure 11, an order of magnitude difference exists between

the injurious fluid temperatures for air and water. The difference between oil and water is not as substantial, but is still about a factor of two for 0.1 second exposure. For exposure times greater than five seconds, the difference in injurious fluid temperatures is minimal, injury here being controlled by tissue conduction rather than convection at the surface.

5. CONCLUSIONS

Analyses of tissue heat transfer during scald events, when applied in conjunction with an appropriate thermal injury criterion, provide a means of extending the results of existing experimental studies, and establishing critical exposure levels for different fluids.

One of the most important considerations in the heat transfer analysis is the determination of the initial tissue temperature, which in turn is dependent on tissue properties and pre-scald convective conditions. For short exposure times, the initial temperature has a major influence on tissue temperature excursions, and therefore strongly affects the thermal injury threshold. With increasing exposure times, however, the effect of the tissue temperature transient on thermal injury diminishes, resulting in a reduction in sensitivity to variations in tissue properties and initial conditions. For fluid exposure times greater than 5 seconds, properties and initial conditions appear to have little or no influence on the injury threshold.

Aside from fluid temperature, the convective heat transfer coefficient for the scalding fluid is undoubtedly the most crucial factor in assessing scald threat. Critical fluid temperatures can easily differ by a factor of two when one considers the wide range of fluid properties and possible flow conditions. The current approach for establishing critical exposure levels is directly applicable to any fluid and flow of concern.

6. REFERENCES

1. Moritz, A. R., Henriques, F. C., Jr., Studies of Thermal Injury: II, The Relative Importance of Time and Surface Temperature in the Causation of Cutaneous Burns, Am. J. Path. 23:695, 1947.

2. Diack, A. W., Schulty, R. D., et al., Technique for Quantifying Low Temperature Burns, JSR, Vol. 4, No. 6, June 1964.

3. Stoll, A. M., Greene, L. C., Relationship Between Pain and Tissue Damage Due to Thermal Radiation, J. Appl. Physiol., Vol. 14, No. 3, May 1959.

4. Stoll, A. M., Chianta, M. A., Burn Production and Prevention in Convective and Radiant Heat Transfer, Aerospace Medicine, Vol. 39, No. 10, October 1968.

5. Stoll, A. M., Chianta, M. A., Method and Rating System for Evaluation of Thermal Protection, Aerospace Medicine, Vol. 40, No. 11, November 1969.

6. Weaver, J. A., Stoll, A. M., NADC Memo Report 6708, 1967.

7. Takata, A., Development of Criterion for Skin Burns, Aerospace Medicine, Vol. 45, No. 6, June 1974.

8. Pennes, H. H., Analysis of Tissue and Arterial Blood Temperatures in the Resting Human Forearm, J. Appl. Physiol., Vol. 1, No. 2, August 1948.

9. Wissler, E. H., A Mathematical Model of the Human Thermal System, Bulletin of Mathematical Biophysics, Vol. 26, 1964.

10. Wissler, E.H., An Analysis of Factors Affecting Temperature Levels in the Nude Human, In: Temperature-Its Measurement and Control in Science and Industry, J. D. Hardy, Ed., Vol. 3, Pt. 3, 1963.

11. Wissler, E. H., Steady-State Temperature Distribution in Man, J. Appl. Physiol., Vol. 16, No. 4, 1961.

12. Shitzer, A., Chato, J. C., Analytical Solutions to the Problem of Transient Heat Transfer in Living Tissue, Trans. ASME, Journal of Biomechanical Engineering, Vol. 100, November 1978.

13. Chato, J. C., Shitzer, A., Analytical Prediction of the Heat Transfer from a Blood Vessel Near the Skin Surface Cooled by a Symmetrical Strip, Trans. ASME, Journal of Engineering for Industry, February 1975.

14. Chato, J. C., and Shitzer, A., On the Dimensionless Parameters Associated with Heat Transport within Living Tissue, Aerospace Medicine, Vol. 41, No. 4, April 1970.

15. Shitzer, A., Chato, J. C., Analytical Modeling of the Thermal Behavior of Living Human Tissue, paper Cu 3.9 presented at the 4th International Heat Transfer Conference, Paris-Versailles, 1970.

16. Chato, J. C., A Method for the Measurement of the Thermal Properties of Biological Materials, Thermal Problems in Biotechnology, ASME Symposium Series, 1968.

17. Rao, P. P., Francis, J. E. et al., Comparison of Analyses and Experiment in Transient Thermographic Studies, AIAA Paper No. 75-712 presented at the AIAA 10th Thermophysics Conference, Denver, Colorado, May 27-29, 1975.

18. Love, T. J., Francis, J. E. et al., A Comparison of Predicted Skin Temperatures with Thermographic Measurements, presented at the Fifth Symposium on Temperature, Washington, D.C., June 21-24, 1971.

19. Wulff, W., The Energy Conservation Equation for Living Tissue, IEEE Trans., Vol. BME-21, No. 6, November 1974.

20. Klinger, H. G., The Description of Heat Transfer in Biological Tissue, Proceedings Conference on Thermal Characteristics of Tumors: Applications in Detection and Treatment, New York Academy of Sciences, March 14-16, 1979.

21. Chen, M. M., Holmes, K. R., Microvascular Contributions in Tissue Heat Transfer, Proceedings Conference on Thermal Characteristics of Tumors: Applications in Detection and Treatment, New York Academy of Sciences, March 14-16, 1979.

22. Henriques, F. C., Jr., Studies of Thermal Injury: V, The Predictability and the Significance of Thermally Induced Rate Processes Leading to Irreversible Injury, Arch. Path., 43:489, 1947.

23. Fugitt, C. E., A Rate Process of Thermal Injury, Armed Forces Special Weapons Project, AFSWP-606, December 6, 1955.

24. Wu, Y. C., A Modified Criterion for Predicting Thermal Injury, Report in Process, National Bureau of Standards, Washington, D.C.

25. Moussa, N. A., McGrath, J. J. et al., Kinetics of Thermal Injury in Cells, Trans. ASME, Journal of Biomechanical Engineering, Vol. 99, August 1977.

26. Lawrence, J. C., Bull, J. P., Thermal Conditions Which Cause Skin Burns, Engineering in Medicine, J. Mech. E., 1976.

27. Rushmer, R. F., Buettner, J. K. et al., The Skin, Science, Vol. 154, No. 3747, October 21, 1966.

28. Jain, R. K., Effect of Inhomogenetics and Finite Boundaries on Temperature Distributions in a Perfused Medium, with Application to Tumors, Trans. ASME, Journal of Biomechanical Engineering, Vol. 100, November 1978.

29. Wu, Y. C., Control of Thermal Impact for Thermal Safety AIAA Journal, Vol. 15, No. 5, May 1977.

30. Reay, D. A., Thiele, F. A. J., Heat Pipe Theory Applied to a Biological System: Quantification of the Role of the "Resting" Eccrine Sweat Gland in Thermoregulation, J. Theor. Biol., Vol. 64, 1977.

31. Richardson, P. D., Whitelaw, J. H., Transient Heat Transfer in Human Skin, Journal of the Franklin Institute, Vol. 286, No. 3, September 1968.

32. Stoll, A. M., Heat Transfer in Biotechnology, in Advances in Heat Transfer, Vol. 4, 1967.

33. Squire, H. B., Modern Developments in Fluid Dynamics 3rd Edition, Vol. 2, Oxford: Clarendon Press, 1950.

34. Weinbaum, S., Jiji, L. M., A Two Phase Theory for the Influence of Circulation on the Heat Transfer in Surface Tissue, ASME Paper No. 79/HT-72, presented at the Winter Annual Meeting, New York, NY, December 2-7, 1979.

35. Perl. W., Heat and Matter Distribution in Body Tissues and the Determination of Tissue Blood Flow by Local Clearance Methods, J. Theor. Biol., Vol. 2, 1962.

36. Wu, Y. C., Rate of Cell Damage in Thermal Injury, NBS-CCPT Report to the Consumer Product Safety Commission, Washington, D.C.

TABLE 1

Typical Properties for Components of Skin[A]

	Thickness mm	Density $\frac{kg}{m^3} \times 10^{-3}$	Specific Heat $\frac{J}{kgK} \times 10^{-3}$	Thermal Conductivity $\frac{w}{mK}$	Thermal Diffusivity $\frac{m^2}{sec} \times 10^{7}$	Rate
Stratum Corneum	0.05	---	---	---	---	---
Epidermis	0.10	1.0	3.3-4.6 (4.2)	0.33-0.63 (0.42)	0.7-1.3 (1.0)	---
Dermis	0.5-0.7	1.2[B]	3.2[B]	0.37[B]	1.0[C]	---
Subdermal Fat	1-4	$\rho c_p = 3.8 \times 10^{-6} \frac{J}{m^3 K}$		0.21	0.7[C]	---
Blood	---	1.0	3.8-4.2 (3.9)	---	---	---
Blood Perfusion	---	---	---	---	---	0.1-7.0 $\frac{kg}{m^3 sec}$ (0.4)
Metabolic Heat Generation	---	---	---	---	---	210-840 $\frac{w}{m^3}$ (420)

A - Taken from References [3, 14, 17, 18, 26-32]

B - Values for porcine tissue

C - Calculated from other reported thermal properties

( ) - Most representative approximate value

TABLE 2

Heat Transfer Coefficients for Various Fluids

Fluid	Fluid Velocity m/sec	Convective Coefficient w/m^2K
Water	0.3	4000
	3.0	12500
Oil	0.3	800
	3.0	2500
Air	0.3	13
	3.0	40

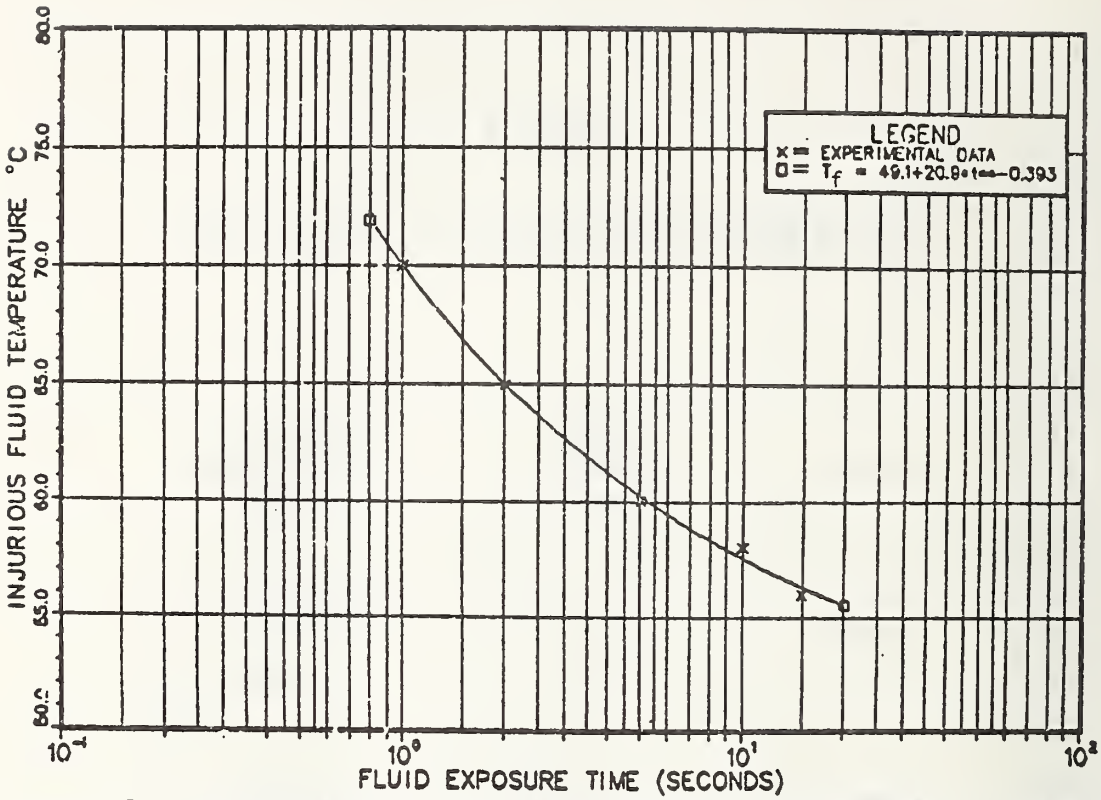

FIGURE 1. INJURY THRESHOLD FOR WATER DETERMINED EXPERIMENTALLY BY MORITZ

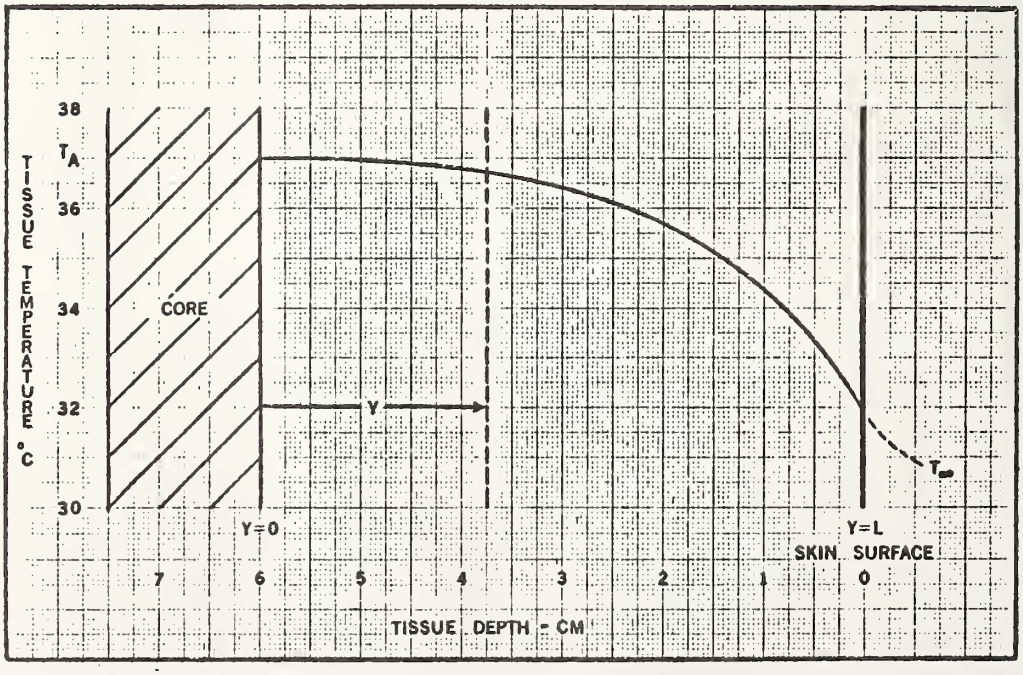

FIGURE 2. INFINITE SLAB MODEL OF SKIN TISSUE AND THE INITIAL TISSUE TEMPERATURE DISTRIBUTION

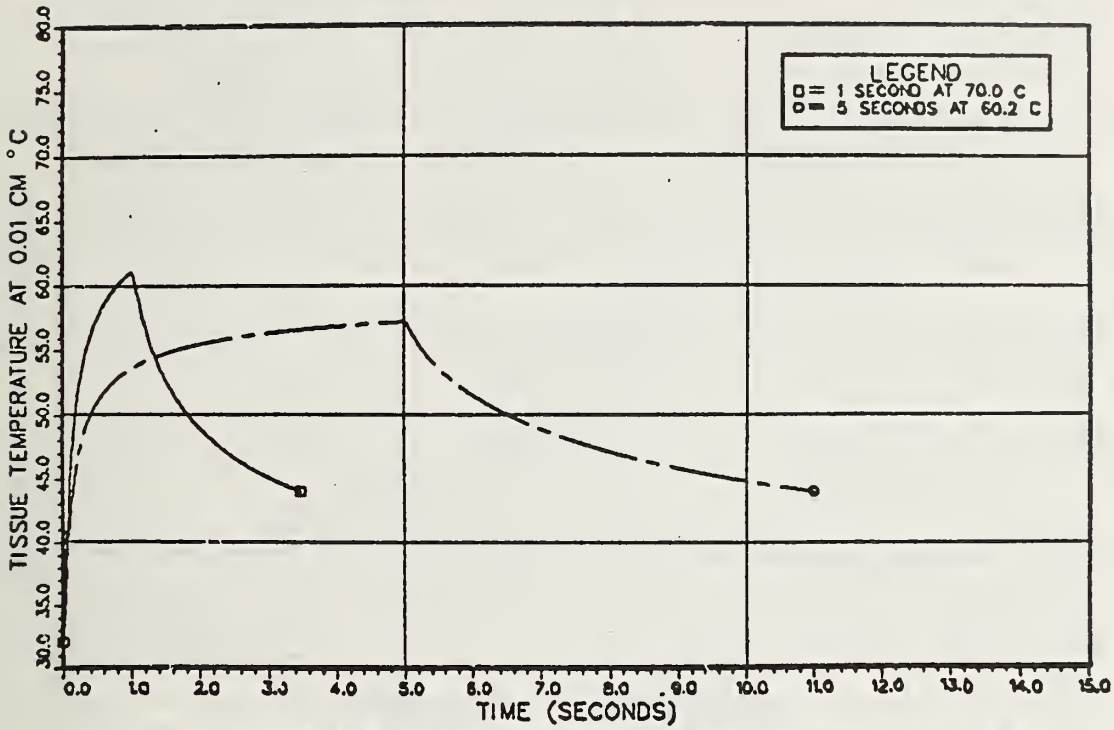

FIGURE 3. TISSUE TEMPERATURE PROFILES FOR TWO FLUID EXPOSURES

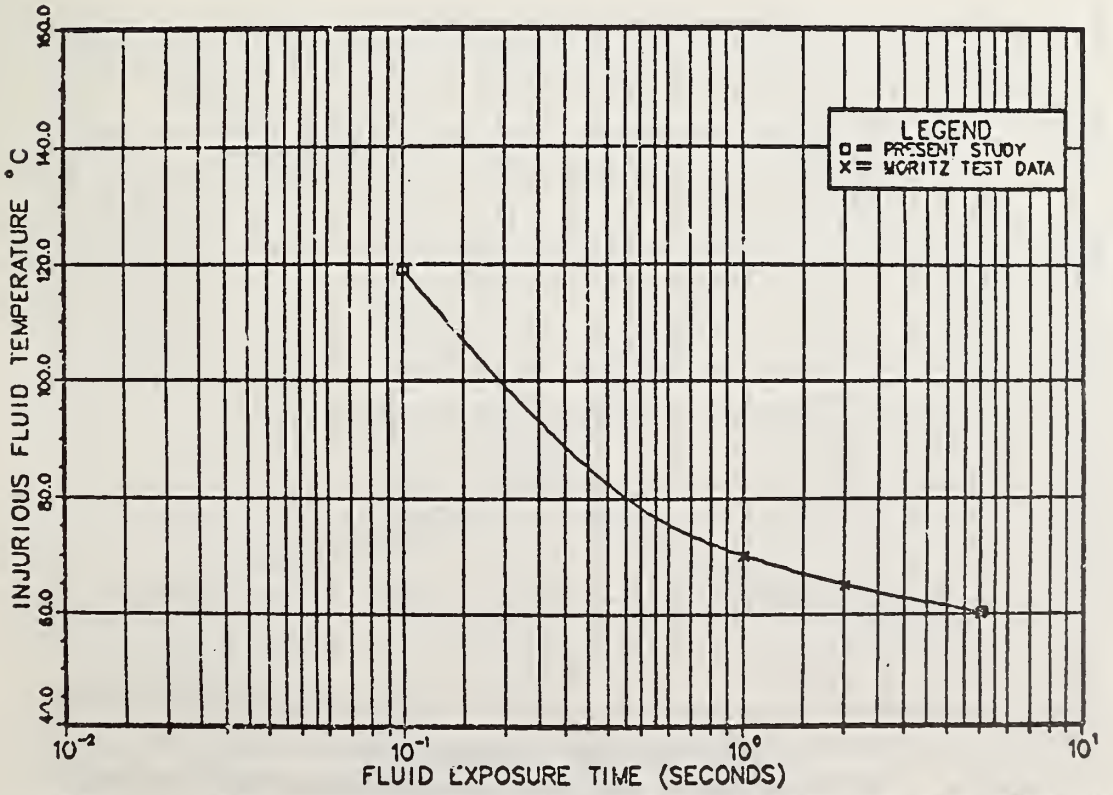

FIGURE 4. INJURY THRESHOLD PREDICTED BY SUBJECT MODEL FOR BASE CASE VALUES

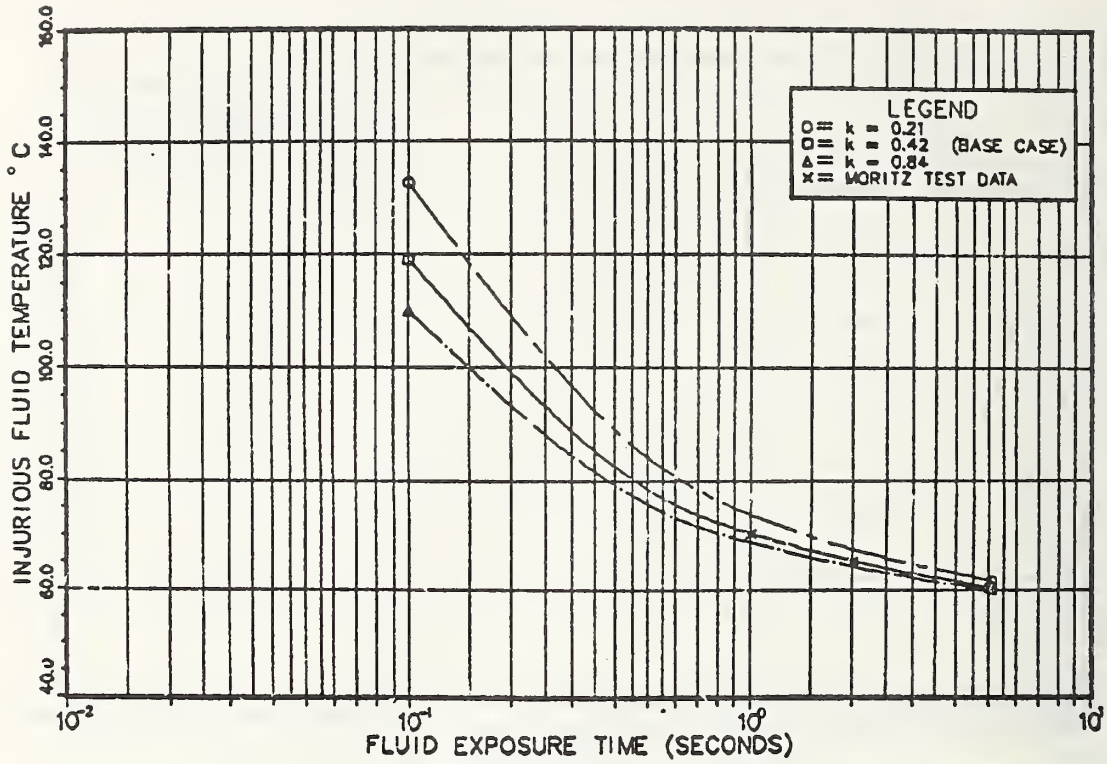

FIGURE 5. EFFECT OF THERMAL CONDUCTIVITY ON THE INJURY THRESHOLD

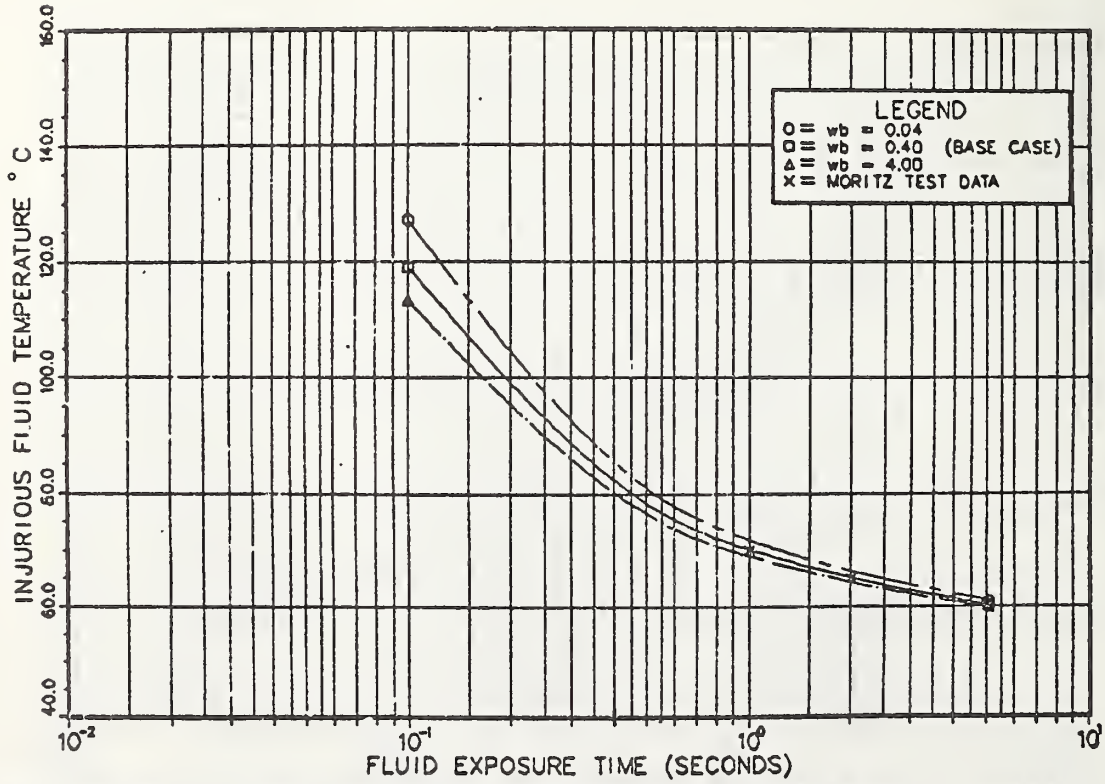

FIGURE 6. EFFECT OF BLOOD PERFUSION RATE ON THE INJURY THRESHOLD

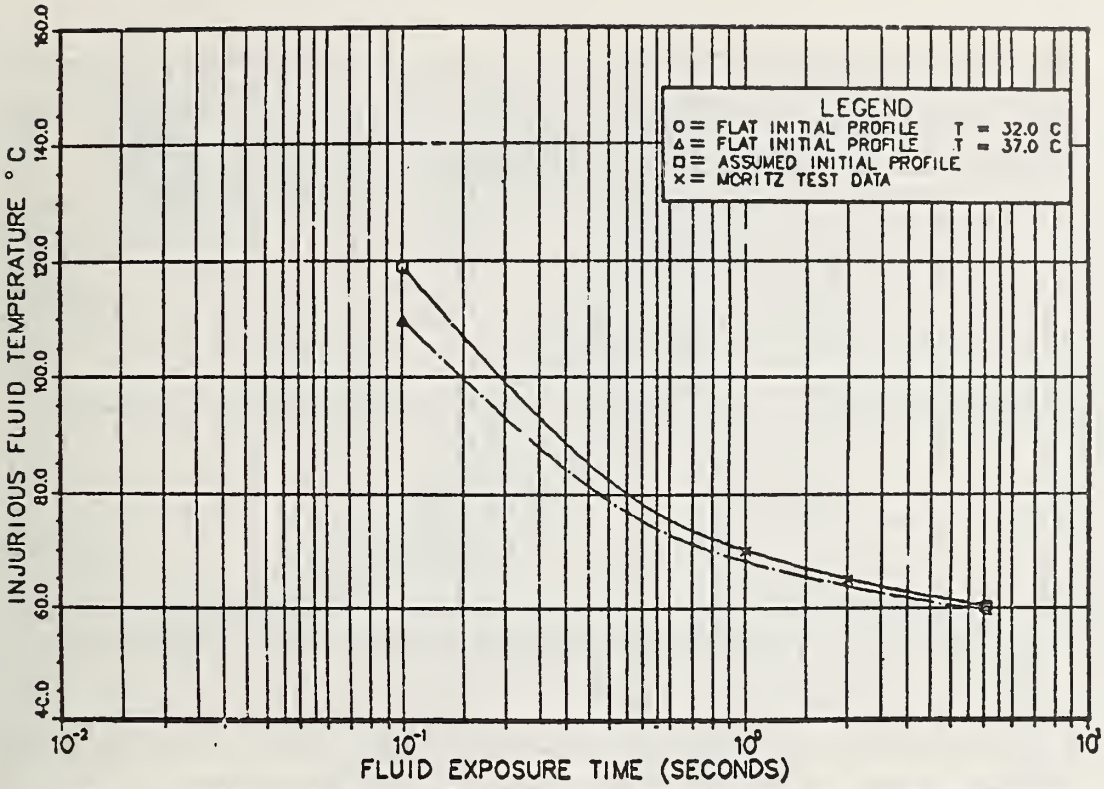

FIGURE 7. EFFECT OF INITIAL TEMPERATURE PROFILE ON THE INJURY THRESHOLD

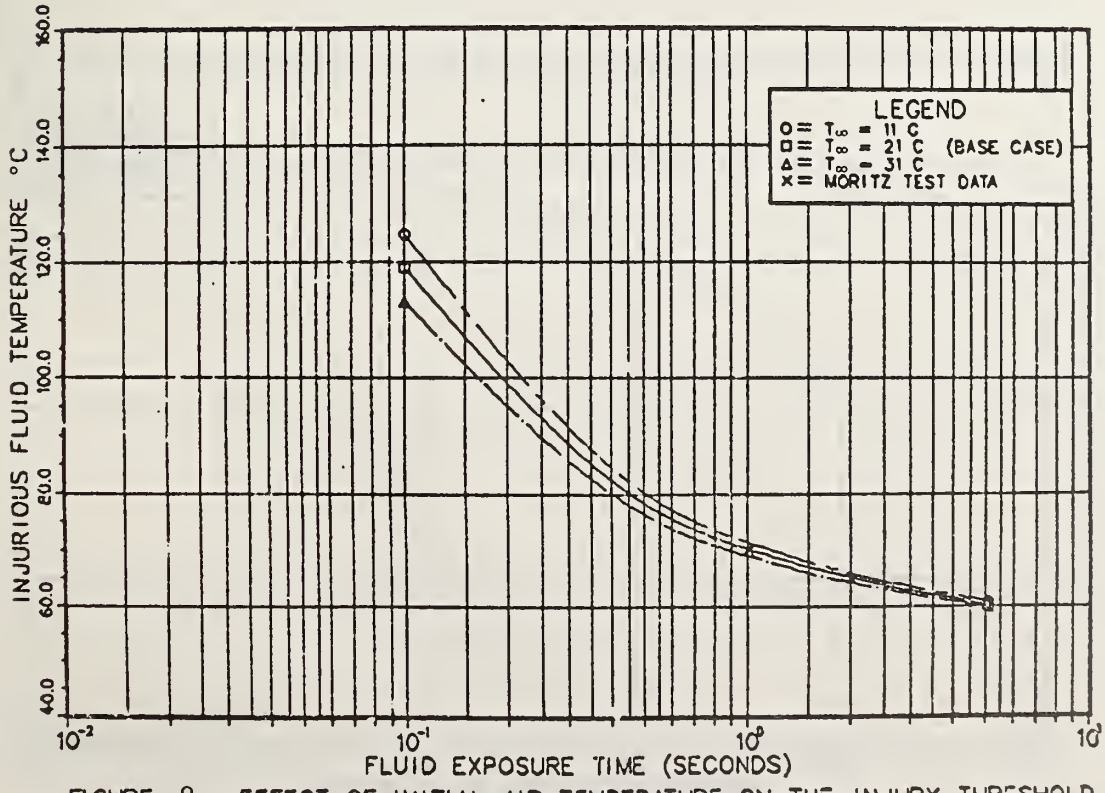

FIGURE 8. EFFECT OF INITIAL AIR TEMPERATURE ON THE INJURY THRESHOLD

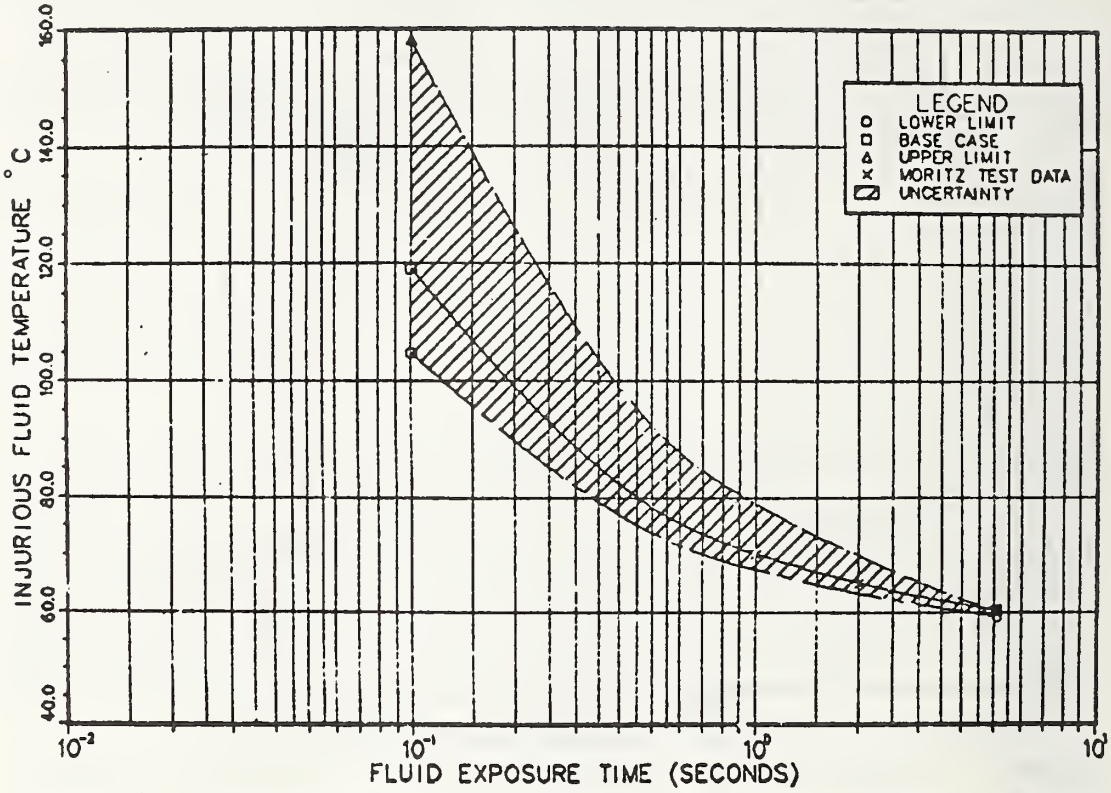

FIGURE 9. THRESHOLD RANGE FOR EXTREME COMBINATIONS OF THERMAL PROPERTIES

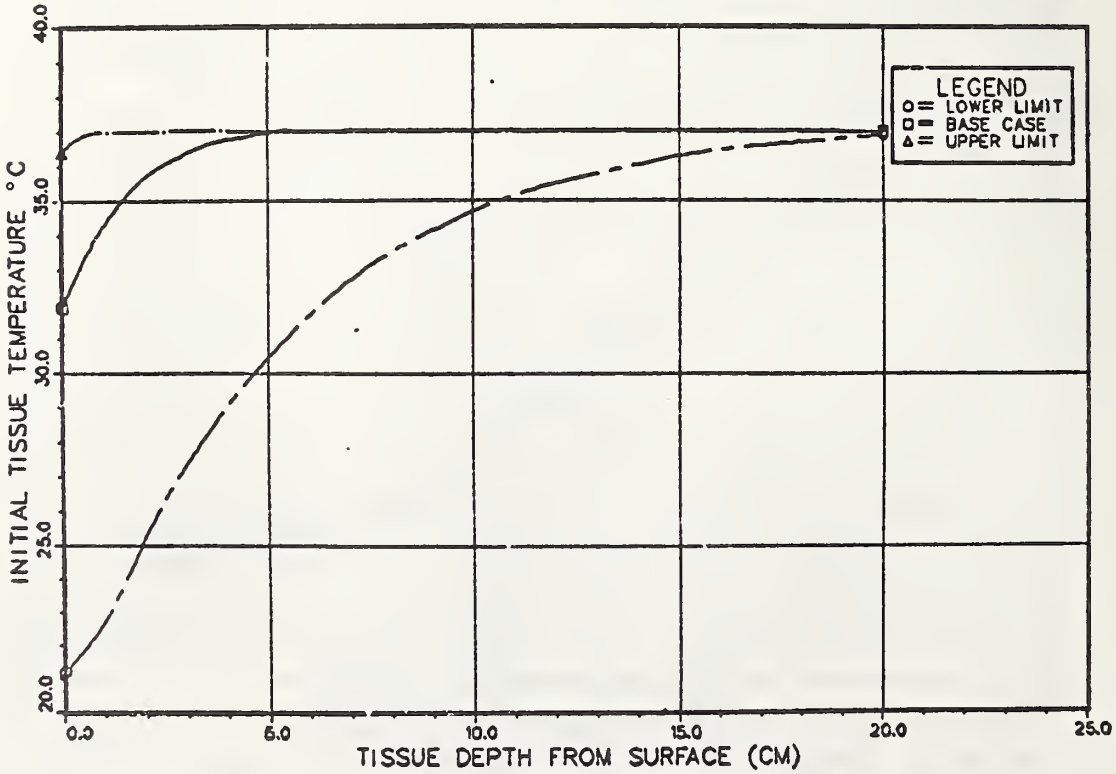

FIGURE 10. INITIAL TEMPERATURE PROFILE FOR COMBINATIONS OF PROPERTIES

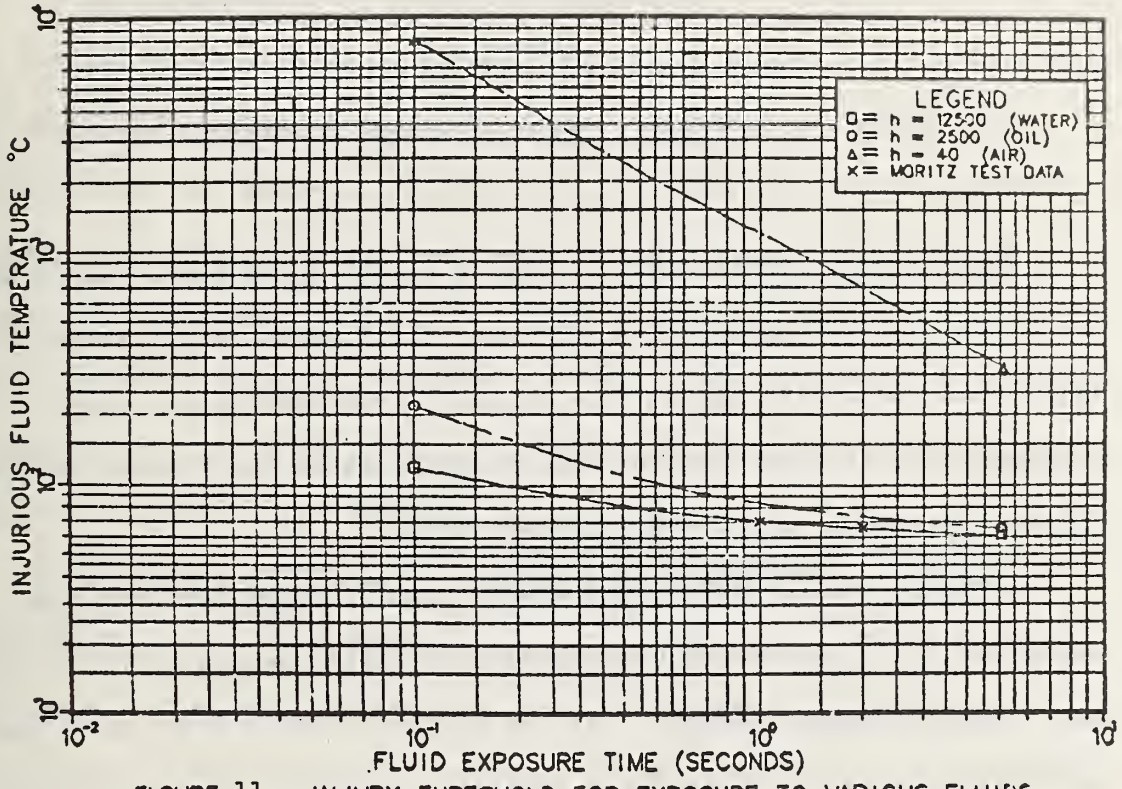

FIGURE 11. INJURY THRESHOLD FOR EXPOSURE TO VARIOUS FLUIDS

Appendix A

Derivation of the Bio-heat Equation

The vascular architecture in living tissue is complex, with dramatic variations in the number, size, spacing, and flow velocity associated with blood vessels throughout the tissue. This complexity poses a fundamental difficulty in the detailed modeling of the thermal interaction between arteries, veins, and perfused tissue.

Although some detailed tissue heat transfer analyses have been conducted [34], additional measurements are still needed to verify the more complex thermal models. For the purpose of this study, a "crude" approximation to the tissue heat transfer problem was therefore utilized. The approximation, to be derived here, combines a local description of the tissue temperature gradients with a global description of the thermal convective effects of the moving blood, which treats the blood phase as a volumetric isotropic heat source.

The temperature field in a continuous, homogeneous medium with constant thermal conductivity can be described by the well-known Fourier heat conduction equation

$$\rho c_p \frac{\partial T}{\partial t} = k \nabla^2 T + q \quad . \tag{A1}$$

If this equation is to apply to a material such as skin tissue, the thermal properties would become "effective" properties, incorporating all the physiological phenomena peculiar to tissue, including blood perfusion and metabolic heat generation. Rather than treat tissue heat transfer using this "lumped" approach, however, Equation A1 can be modified to separately account for these phenomena. To do this, additional terms must be introduced. These terms are developed through consideration of a small volume of tissue, ΔV, perfused by blood, and application of Fick's Principle.

The vascular network in a tissue is idealized into a system of circulatory loops, as shown in figure A1. Each loop consists of three functional components denoted arteriole, capillary, and venule (A, C, and V in figure A1 respectively). The capillary is that portion of the loop in which all exchange (of a substance or heat) between the flowing blood and the surrounding tissue is assumed to take place. The arteriole is the portion of the loop in which blood flows toward the capillary and, conversely, the venule is the portion in which blood flows away from the capillary. It is assumed that no exchange between blood and tissue takes place in these two portions. Although strictly speaking, heat transfer in the arteriole and venule are not negligible, the diameter of a capillary is so minute relative to its length (5×10^{-4} cm versus 0.1 cm) that as a heat exchanger its effectiveness is near unity; it is therefore credited for all heat transfer.

The substance of interest, heat in our case, can enter and leave the volume element by perfusion in either of two ways: (a) entry through

arterioles terminating within the volume and exit through venules starting from within the volume element and (b) entry or exit through capillaries intersecting the surface of the volume element. Vessels of Type (a) are those in which the capillary is enclosed within the element, such as I, II, and IV of figure A1. Type (b) vessels comprise the remainder (III, V, VI, and VII) and are referred to as surface capillaries. The heat transfer contributions of both vessel types are different and must be dealt with separately.

Type (a) Vessels

The contribution of Type (a) vessels can be derived via Fick's Principle of Perfusion for an Organ. For the element ΔV, Fick's equation may be written:

$$\left(\frac{\partial \Delta C}{\partial t}\right)_{p(a)} = \phi_a C_a - \phi_v C_v \qquad \text{(A2)}$$

where ΔC is the concentration of substance in the volume element in kg/m^3, ϕ is the blood perfusion rate in sec^{-1}, and C is the concentration of substance in the blood, kg/m^3. The subscripts a and v denote the arterial and venous conditions respectively. For the substance of interest, heat, concentration is equivalent to thermal energy per unit volume, or the product of density, specific heat, and temperature. Hence, for heat flow, Equation A2 becomes

$$\rho c_p \left(\frac{\partial T}{\partial t}\right)_{p(a)} = \rho_b c_{pb} \left(\phi_a T_a - \phi_v T_v\right) . \qquad \text{(A3)}$$

In the absence of blood accumulation or depletion in ΔV, $\phi_a = \phi_v = \phi$. Also, based on the existing idea that exchange in a capillary occurs predominantly in its initial portion, the venous temperature can be assumed equal to the local tissue temperature, that is, $T_v = T$. Incorporating these approximations and letting $w_b = \rho_b \phi$, kg/m^3 sec, Equation A4 can finally be written

$$\rho c_p \left(\frac{\partial T}{\partial t}\right)_{p(a)} = w_b c_{pb} (T_a - T) \quad . \tag{A4}$$

Fick's perfusion equation comprises only contributions from Type (a) vessel loops in which the capillaries are contained entirely within the volume element. Type (b) vessel loops have capillaries which intersect the surface of the element. The contribution of these vessels to the rate of change in thermal energy of the element is in addition to that given by Equation A4.

Type (b) Vessels

To derive the effect of surface capillaries, consider the flow of blood in the capillaries intersecting the right hand $\Delta Y\ \Delta Z$ face of ΔV (figure A1). Letting j_{x+} denote the flux density of blood in the positive x direction (path III) and j_{x-} denote that in the negative x direction (path VI), the net rate of inflow of substance across the face is

$$(j_{x-} C_{b-} - j_{x+} C_{b+})\ \Delta Y\ \Delta Z \tag{A5}$$

where C_{b-} and C_{b+} denote the average concentrations of substance in the respective vessels. In thermal energy notation, concentration is again equivalent to the product of density, specific heat, and temperature. Equation A5 then takes the form

$$(j_{x-} \rho_b c_{pb} T_{b-} - j_{x+} \rho_b c_{pb} T_{b+}) \Delta Y \Delta Z . \quad (A6)$$

Since the heat exchange in a capillary occurs predominantly in its initial portion, it is in near-equilibrium with its surroundings along most of its length. T_{b-} and T_{b+} can, therefore, be assumed equal to the local tissue temperature T. Letting $j_x = j_{x+} - j_{x-}$, the net rate of heat inflow through the right $\Delta Y \Delta Z$ face is

$$-\rho_b c_{pb} (j_x T) \Delta Y \Delta Z . \quad (A7)$$

The difference in flux between the left and right hand $\Delta Y \Delta Z$ faces may be expressed as the product of the partial of Equation A7 with respect to x and the length of the element in the x direction, ΔX. The result is

$$-\rho_b c_{pb} \frac{\partial (j_x T)}{\partial x} \Delta X \Delta Y \Delta Z . \quad (A8)$$

Similar terms can be derived for flows through the $\Delta X \Delta Z$ and $\Delta X \Delta Y$ faces (y and z flow directions respectively). The sum of these terms represents the rate of heat gain of the element ΔV due to all surface

capillaries. This contribution may be written

$$\rho c_p \left(\frac{\partial T}{\partial t}\right)_{p(b)} = -\rho_b \, c_{pb} \left(\frac{\partial (j_x T)}{\partial x} + \frac{\partial (j_y T)}{\partial y} + \frac{\partial (j_z T)}{\partial z}\right)$$

$$= -\rho_b \, c_{pb} \, \nabla(jT) \, . \tag{A9}$$

Collecting terms on the left hand sides of Equations A1, A4, and A9 yields the complete partial differential equation for tissue heat transfer:

$$\rho c_p \frac{\partial T}{\partial t} = k\nabla^2 T - \rho_b \, c_{pb} \, \nabla(jT) + w_b \, c_{pb} \, (T_a - T) + q \, . \tag{A10}$$

That the effect of the surface capillary term is small can be shown by considering the one-dimensional steady state case with zero metabolic heat generation. Letting $\theta = T - T_a$ and $\chi = k/\rho_b \, c_{pb}$, Equation A10 becomes:

$$\chi \frac{d^2\theta}{dx^2} - j_x \frac{d\theta}{dx} - \phi\theta = 0 \, . \tag{A11}$$

The solution to Equation A11 subject to the boundary conditions

$$\theta \, (x = 0) = \theta$$

$$\theta \, (x = \infty) = \text{real}$$

is

$$\theta = \theta_s \, e^{-\frac{\sqrt{j_x^2 + 4\chi\phi} - j_x}{2\chi} x} \quad . \tag{A12}$$

The maximum possible j exists when all the capillaries are uniformly aligned and the blood flows in the x direction, as in vessels IV, V, and VI of figure A1. In this case, the density vector j is

$$j_x = \ell\phi \tag{A13}$$

where ℓ is a vector of the magnitude of the average capillary length and in the direction of the capillary net blood flow [35].

The relative insignificance of the surface capillary effect can be seen by introducing this expression into Equation A12 and comparing the magnitudes of the two terms under the square root sign. The ratio of the first term to the second is

$$\frac{j_x^2}{4\chi\phi} = \frac{\ell^2\phi}{4\chi} \quad . \tag{A14}$$

Assuming approximate values for these parameters [35]:

$$\ell = 0.001 \text{ m},$$

$$\phi = 0.01 \text{ sec}^{-1}, \text{ and}$$

$$\chi = 1.2 \times 10^{-7} \text{ m}^2/\text{sec}$$

gives $\ell^2\phi/4\chi = 0.02$. It thus appears that the surface capillary effect is insignificant. This same conclusion can be arrived at by assuming that the capillaries are sufficiently random in arrangement and direction that they exhibit no preferred direction.

Neglecting the contribution of surface capillaries, Equation A10 reduces to its final form:

$$\rho c_p \frac{\partial T}{\partial t} = k\nabla^2 T + w_b c_{pb} (T_a - T) + q \tag{A15}$$

or alternatively:

$$\frac{1}{\alpha} \frac{\partial T}{\partial t} = \nabla^2 T + \frac{w_b c_{pb}}{k} (T_a - T) + \frac{q}{k} \tag{A16}$$

where α is the thermal diffusivity of tissue. This is the so-called bio-heat equation first applied by Pennes [8] to determine the temperature distribution in the human forearm.

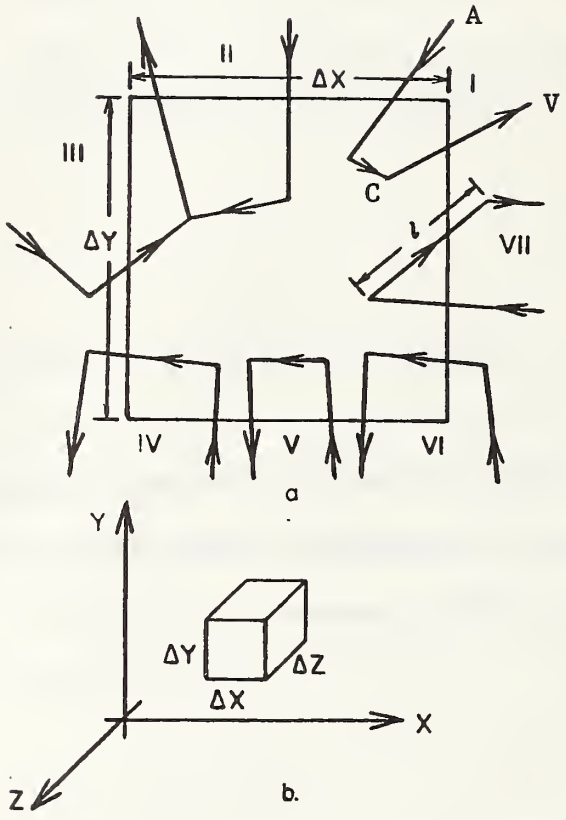

FIGURE A1. VOLUME ELEMENT OF TISSUE INTERSECTED BY VARIOUS PATHS OF CAPILLARY BLOOD FLOW [35]

Appendix B

Finite Difference Formulation for Tissue Heat Transfer During Scalding

The scald problem requires that the time-temperature history of the skin tissue at a depth of approximately 0.01 cm be known over the complete scald event -- heating and cooling -- so that the severity of scalding can be assessed via a thermal injury criterion. Because the tissue is subject to an initial temperature distribution as well as to different sets of convective boundary conditions for the heating and cooling periods, a finite difference solution is the most expedient means of obtaining the required temperature profile.

The finite difference formulation used in this study is an implicit type. An energy balance for each selected node in the tissue is written. The resulting set of equations for the "future" temperature of each node is then assembled in matrix form and solved simultaneously via matrix techniques.

Governing Equation

The governing partial differential equation for tissue heat transfer is the bio-heat equation, described in detail in Appendix A. This equation is the Fourier heat conduction equation with an additional term, $-w_b c_{pb}(T-T_a)$, to account for heat transport by perfusing blood. Here w_b and c_{pb} refer to the perfusion rate and specific heat of blood, while T and T_a are the local tissue temperature and fixed arterial temperature respectively.

For this analysis, one-dimensional heat flow is assumed. Also, all thermal properties throughout the tissue, including blood flow parameters, are considered constant.

Boundary conditions for the problem are: convection at the tissue surface, and a constant arterial temperature at some finite depth below the surface. The initial condition is the tissue temperature distribution defined by Equation 18 in the text.

Node Configuration

Thermal injury criterion requires that temperature at a depth of 0.01 cm be known, but we also want the temperature at the deepest node to remain constant during the heating and cooling event. Division of the tissue into two regions facilitates this. In the first region, Region A of figure B1, nodes are closely spaced such that one node may lie at a depth of 0.01 cm. In the second region, Region B, a sufficiently large depth, DB, may be selected such that the temperature of the last node, BL, remains constant throughout the scald event. The node spacing in Regions A and B, ΔX_A and ΔX_B respectively, may be chosen to minimize the number of nodes required.

Node Equations

An energy balance must be written for each node in the tissue. For the nth node, the general form of the energy balance or node equation is:

$$(T_n^{t+1} - T_n^{t})\, C_n = \Delta t \left[\frac{T_{n-1}^{t+1} - T_n^{t+1}}{R_{n-1,n}} + \frac{T_{n+1}^{t+1} - T_n^{t+1}}{R_{n,n+1}}\right.$$

$$\left. - w_b c_{pb}\, \Delta V_n\, (T_n^{t+1} - T_a) + q_n\, \Delta V_n\right] \qquad \text{(B1)}$$

where the thermal capacitance $C = \rho c_p A \Delta X$. Thermal resistance, R, for convection between the surface node and ambient air is given by

$$R = 1/hA \qquad \text{(B2)}$$

while for conduction between the surface node and all interior nodes it is given by

$$R = \Delta X/kA\ . \qquad \text{(B3)}$$

The temperature at most tissue nodes may be expressed using the same form of Equation B1; however, different equations are needed for the surface node and the two nodes at the Region A-Region B interface. In all, a total of five different forms of Equation B1 are necessary. Each form applies to similar types of nodes; these are:

1) surface node
2) all interior nodes in Region A
3) last node in Region A
4) first node in Region B
5) all interior nodes in Region B .

The temperature of the last node in Region B (Node BL) is a specified constant temperature, namely, the arterial temperature.

The particular equations for the future or updated temperature for each of the node types are as follows:

Surface Node (Node 1):

$$T_1^{t+1}\left[1 + \frac{2\Delta t}{\rho c_p \Delta X_A}\left(h + \frac{k}{\Delta X_A} + w_b c_b \frac{\Delta X_A}{2}\right)\right] + T_2^{t+1}\left[-\frac{2\alpha\Delta t}{\Delta X_A^2}\right]$$

$$= \frac{2h\Delta t}{\rho c_p \Delta X_A} T_\infty + \frac{\Delta t}{\rho c_p}(w_b c_b T_a + q) + T_1^t . \tag{B4}$$

All interior Nodes in Region A (Nodes A):

$$T_{A-1}^{t+1}\left[-\frac{\alpha\Delta t}{\Delta X_A^2}\right] + T_A^{t+1}\left[1 + 2\frac{\alpha\Delta t}{\Delta X_A^2} + \frac{w_b c_b \Delta t}{\rho c_p}\right.$$

$$\left. + T_{A+1}^{t+1}\left[-\frac{\alpha\Delta t}{\Delta X_A^2}\right]\right. = \frac{\Delta t}{\rho c_p}(w_b c_b T_a + q) + T_A^t . \tag{B5}$$

Last Node in Region A (Node AL):

$$T_{AL-1}^{t+1}\left[-\frac{\alpha\Delta t}{\Delta X_A^{\,2}}\right]+T_{AL}^{t+1}\left[1+\frac{\alpha\Delta t}{\Delta X_A^{\,2}}+\frac{2\alpha\Delta t}{\Delta X_A(\Delta X_A+\Delta X_B)}+\frac{w_b c_b \Delta t}{\rho c_p}\right]$$

$$+T_{B1}\left[-\frac{2\alpha\Delta t}{\Delta X_A(\Delta X_A+\Delta X_B)}\right]=\frac{\Delta t}{\rho c_p}(w_b c_b T_a+q)+T_{AL}^{t}\,. \tag{B6}$$

First Node in Region B (Node B1):

$$T_{AL}^{t+1}\left[-\frac{2\alpha\Delta t}{\Delta X_B(\Delta X_A+\Delta X_B)}\right]+T_{B1}^{t+1}\left[1+\frac{2\alpha\Delta t}{\Delta X_B(\Delta X_A+\Delta X_B)}+\frac{\alpha\Delta t}{\Delta X_B^{\,2}}+\frac{w_b c_b \Delta t}{\rho c_p}\right]$$

$$+T_{B1+1}^{t+1}\left[-\frac{\alpha\Delta t}{\Delta X_B^{\,2}}\right]=\frac{\Delta t}{\rho c_p}(w_b c_b T_a+q)+T_{B1}^{t}\,. \tag{B7}$$

All Interior Nodes in Region B (Nodes B):

$$T_{B-1}^{t+1}\left[-\frac{\alpha\Delta t}{\Delta X_B^{\,2}}\right]+T_{B}^{t+1}\left[1+2\,\frac{\alpha\Delta t}{\Delta X_B^{\,2}}+\frac{w_b c_b \Delta t}{\rho c_p}\right]$$

$$+T_{B+1}^{t+1}\left[-\frac{\alpha\Delta t}{\Delta X_B^{\,2}}\right]=\frac{\Delta t}{\rho c_p}(w_b c_b T_a+q)+T_{B}^{t}\,. \tag{B8}$$

For the last node in Region B (Node BL) select depth sufficiently deep that $T_{BL} = T_a$. Rearranging and replacing parameter groups with constants, Equations B4 and B8 may be expressed:

$$T_1^{t+1} + C1\ T_2^{t+1} = C2\ T_1^{t} + C3\ T_\infty + C4 \qquad \text{(B9)}$$

$$C5\ T_{A-1}^{t+1} + T_A^{t+1} + C5\ T_{A+1}^{t+1} = C6\ T_A^{t} + C7 \qquad \text{(B10)}$$

$$C8\ T_{AL-1}^{t+1} + T_{AL}^{t+1} + C9\ T_{B1}^{t+1} = C10\ T_{AL}^{t} + C11 \qquad \text{(B11)}$$

$$C12\ T_{AL}^{t+1} + T_{B1}^{t+1} + C13\ T_{B1+1}^{t+1} = C14\ T_{B1}^{t} + C15 \qquad \text{(B12)}$$

$$C16\ T_{B-1}^{t+1} + T_B^{t+1} + C16\ T_{B+1}^{t+1} = C17\ T_B^{t} + C18 \quad . \qquad \text{(B13)}$$

Equations B9 through B13, along with the requirement that $T_{BL} = T_a$, may now be assembled in matrix form

$$AX = b \qquad \text{(B14)}$$

where A is a tri-diagonal matrix of C coefficients, X is the vector of updated temperatures (time t+1), and b is the vector of known temperature (time t) and constants. The assembled matrices are shown in figure B2.

The X vector can be solved by inverting the A matrix once and multiplying by b each time step or by use of other matrix techniques.

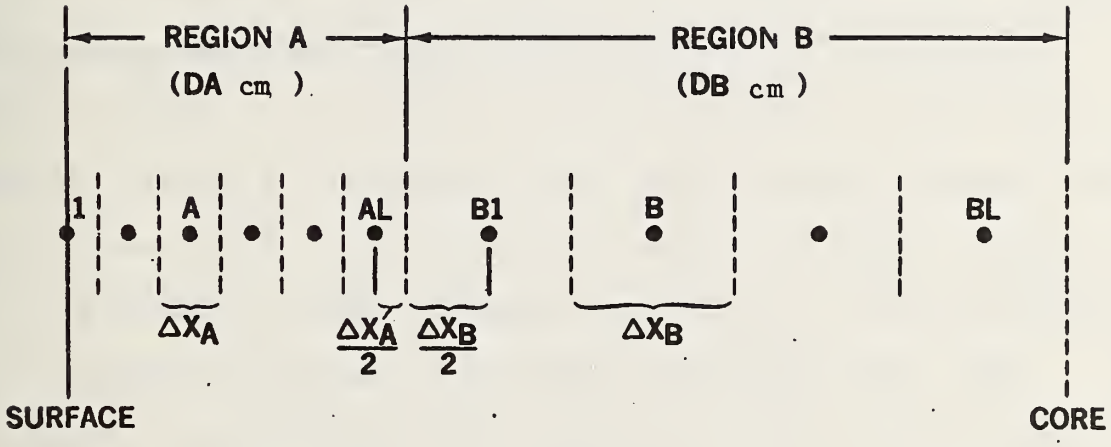

FIGURE B1. TISSUE NODE CONFIGURATION

FIGURE B2. ASSEMBLED MATRICES FOR IMPLICIT FINITE DIFFERENCE SOLUTION

$$
\begin{bmatrix}
1 & C1 & 0 & & & & & & & \\
C5 & 1 & C5 & 0 & & & & & & \\
0 & C5 & 1 & C5 & 0 & & & & & \\
 & 0 & C5 & 1 & C5 & 0 & & & & \\
 & & 0 & C8 & 1 & C9 & 0 & & & \\
 & & & 0 & C12 & 1 & C13 & 0 & & \\
 & & & & 0 & C16 & 1 & C16 & 0 & \\
 & & & & & 0 & C16 & 1 & C16 & 0 \\
 & & & & & & 0 & C16 & 1 & C16 \\
 & & & & & & & 0 & 1 &
\end{bmatrix}
\cdot
\begin{bmatrix}
T_1^{t+1} \\ T_2^{t+1} \\ T_3^{t+1} \\ T_4^{t+1} \\ T_5^{t+1} \\ T_6^{t+1} \\ T_7^{t+1} \\ T_8^{t+1} \\ T_9^{t+1} \\ T_{10}^{t+1}
\end{bmatrix}
=
\begin{bmatrix}
C2\ T_1^t + C3\ T_\infty + C4 \\
C6\ T_2^t + C7 \\
C6\ T_3^t + C7 \\
C6\ T_4^t + C7 \\
C10\ T_5^t + C11 \\
C14\ T_6^t + C15 \\
C17\ T_7^t + C18 \\
C17\ T_8^t + C18 \\
C17\ T_9^t + C18 \\
T_a
\end{bmatrix}
$$

Appendix C

Development of the Thermal Injury Criterion

The living cells in the skin are composed primarily of proteins. These proteins possess disulfide linkages, salt bridges, hydrogen bonds, or combinations of these to form the structural network [36]. All of these chemical bonds are subject to breakage via exposure to thermal energy in excess of the bond strength. When breakage occurs, the protein is inactivated or destroyed. It is recognized that cellular death follows the thermal inactivation of a critical fraction of the protein molecules in the cells of the skin. The point at which tissue damage is observed on a macroscopic scale is not distinct, however, because skin proteins vary in their sensitivity to heat. For example, collagen is not appreciably degraded at temperatures below 71 °C, whereas certain enzyme systems are sensitive to much lower temperatures [26]. The situation is further complicated by the fact that skin cells adjacent to the obviously heat coagulated tissue observed in many burns may not become completely necrotic until several days after injury [26].

Thermal Injury Model

It has been postulated by Henriques [22] and others that the reaction leading to the death of tissue cells conforms to that of most chemical and physical rate processes. The kinetics of a rate process depends on the total energy content of the constituents involved. If this energy content is less than a certain critical value, known as the

activation energy, the process cannot take place. If, on the other hand, the energy content is greater than this critical value, the process takes place and proceeds at a rate proportional to the fraction of the constituents which possess an energy at least equal to the activation energy. This fraction is given by a form of the Maxwell-Boltzman energy distribution law:

$$\frac{n_E}{n} = \exp\,[-\,E/RT]\ . \qquad \text{(C1)}$$

The rate at which the reaction proceeds can be described as:

$$\frac{dn}{dt} = -\,\kappa n\ . \qquad \text{(C2)}$$

In addition to the requirement that energy content be greater than activation energy, steric or spatial requirements for the molecular reaction must also be met before the reaction proceeds. Letting P equal the number of the necessary steric events occurring in one second, and the factor exp [- E/RT] the probability that the particular molecules affected by the steric events also possess the required reaction energy, we may write the reaction rate as the product, or:

$$\frac{dn}{dt} = -\,\kappa n = P \exp\,[-\,E/RT]\ . \qquad \text{(C3)}$$

The number of molecules which will react in a given time is obtained by integrating Equation C3 with the result:

$$n = \int_{t_1}^{t_2} P \exp [- E/RT] \, dt \, . \qquad (C4)$$

Knowing the time-temperature history of skin tissue resulting from a scald event, the number of damaged cells and hence the severity of thermal injury could be assessed via Equation C4. But a detailed knowledge of each of the constituents involved in the reaction, including activation energies, rate constants, etc., would first be necessary in order to evaluate P and E.

In view of the difficulty in specifying the number of cells or even the molecular species involved in the injury process, a different approach is generally taken in applying the rate process concept of Equation C4. The approach is as follows.

If the reaction leading to thermal injury does indeed conform to that of most chemical and physical rate processes, the rate at which damage is inflicted should be given by an expression of the same form as Equation C3. Replacing n in Equation C3 by the parameter Ω, an arbitrary measure of "damage," the damage rate is

$$\frac{d\Omega}{dt} = P \exp [- E/RT_t] \, . \qquad (C5)$$

Integration of Equation C5 gives the total "damage" inflicted over an interval:

$$\Omega = \int_{t_1}^{t_2} P \exp [- E/RT_t] \, dt \, . \qquad (C6)$$

Defining $\Omega = 1$ at the level of inflicted damage just sufficient to destroy cells in the basal layer of the epidermis (partial thickness burn), P and E are then evaluated numerically from experimental observations.

Determination of Empirical Constants

Several researchers have investigated the relationship between the time-temperature history of skin tissue and resulting thermal injury. For convective heat transfer, the original and most widely noted work is that of Moritz et al. [1]. This work involved the study of the relationship between times of exposure to flowing hot water at various temperatures and the occurrence of thermal injury. Their experimental results are presented graphically in figure 1 of the text. Each point along this line represents a different set of scald conditions; however, the result of exposure to these conditions is the same, that is, destruction of cells in the basal layer of the skin or $\Omega = 1$. It should be noted that this curve is valid only for fluid flows similar to that used by Moritz.

In determining the empirical constants P and E, Henriques [22] assumed tissue temperature, T_t, time-invariant and integrated Equation C6 from zero to the end of the heating period (neglecting the cooldown portion of the scald event). Through these assumptions and the selection of a constant value of 1.0 for the scald threshold, Equation C6 becomes:

$$\ell n\ t = E/R \cdot 1/T_t - \ell n\ P\ . \qquad (C7)$$

A plot of Equation C7 for the test data of Moritz showed a linear relationship below T_t = 55 °C from which the constants P = 3.1 x 10^{98} and E = 150000 were determined. The result is a good fit of theory and experimental data for times greater than five minutes, but increasing error for short times typical of scalding (less than five seconds).

Evaluation of Henriques' criterions over the cooling as well as the heating portion of the scald event does not offer much better agreement. Selecting five different exposure conditions from the original data set of Moritz, table C1, the corresponding time-temperature history of skin tissue can be generated using the solution technique described in the text. Evaluating Henriques' criterion over these profiles results in the Ω values given in table C2. These values indicate that Henriques' injury criterion even when evaluated over the entire heating and cooling profile is still lacking for short time exposures. Table C2 values also show that a considerable amount of thermal injury inflicted during a scald event occurs in the cooldown period -- 25% for one second exposures.

Fugitt [23] attempted to resolve the discrepancy between theory and data for short times through an extension of Henriques' criterion. He proposed a two-component thermal degradation process and fitted the original test data with a second line for T_t greater than 55 °C. This yielded values for P and E of 5 x 10^{45} and 70,800 respectively for T_t greater than 55 °C. Unfortunately, this analysis also neglects the cooling portion and does not offer much improvement over the original criterion.

Research similar to that or Moritz and Henriques was also conducted for thermal radiation injury [3-7]. Criteria of the same form as Henriques' was used to describe this type of thermal insult. Weaver et al. [6] used the damage rates:

$$2.185 \times 10^{124} \exp [-93534.9/T_t] \text{ for } 44<T_t<50 \text{ °C}$$

and

$$1.823 \times 10^{51} \exp [-39109.8/T_t] \text{ for } T_t \geq 50 \text{ °C} .$$

Takata [7] found that the damage rates which best fit his test data were:

$$4.322 \times 10^{64} \exp [-50{,}000/T_t] \text{ for } 44 < T_t < 50 \text{ °C}$$

and

$$9.389 \times 10^{104} \exp [-80{,}000/T_t] \text{ for } T_t \geq 50 \text{ °C} .$$

Again, as shown in table C2, agreement between criteria and experiment is not good.

Wu [24] most recently utilized an averaging technique to obtain a tissue temperature-dependent expression for activation energy E. The result

$$E = 150000 - 122(T_t - 53) \text{ for } T_t > 53.0 \text{ °C}$$

gives good agreement between the injury criterion and the original test data (see table C2). This modification was adopted for use in the present study. The complete thermal injury criterion is then:

$$\Omega = P \cdot \int_{t_1}^{t_2} \exp\,[-E/RT_t]\,dt \qquad (C8)$$

where

Ω = the damage integral, 1.0 for partial thickness burn,

P = a constant, 3.1×10^{98} sec^{-1},

E = activation energy, cal/mol,

= 150,000 for $T_t \leq 53.0$ °C,

= 150,000 - 122 $(T_t - 53.0)$ for $T_t > 53.0$ °C,

R = gas constant, 2 cal/K mol,

T_t = tissue temperature at a depth of 0.008 cm, K,

t_1 = time at which T_t = 44.0 °C during heating, sec, and

t_2 = time at which T_t = 44.0 °C during cooling, sec.

Note that Henriques used a tissue depth, x, of 0.008 cm (the thickness of the epidermis) and thermal diffusivity, α, of 0.00071 cm^2/sec, then worked with the quantity $x/2\sqrt{\alpha} = 0.15$. Here we have let x = 0.01 cm and α = 0.001 cm^2/sec. The corresponding quantity $x/2\sqrt{\alpha}$ is only slightly different from Henriques'.

TABLE C1

Exposure Time (sec)	Fluid Temperature (°C)	Corrected Fluid Temperature*, T_f (°C)
1	70	70.0
2	65	65.0
5	60	60.2
10	58	57.5
15	56	56.3

*Based on the non-linear best fit:

$$T_f = 49.08 + 20.91 \times t^{-0.3928}$$

TABLE C2

Thermal Injury Predictions Using Various Injury Criteria

Investigator	Temperature Range (°C)	Injury Criterion Constants P	E	Thermal Injury, Ω, for Various Exposures: 1 sec @ 70°C Heating	Cooling	Total	2 sec @ 65°C Heating	Cooling	Total	5 sec @ 60.2°C Heating	Cooling	Total	10 sec @ 57.5°C Heating	Cooling	Total	15 sec @ 56.3 Heating	Cooling	Total
Henriques[22]	All T_t	3.1×10^{98}	150,000	2.34	0.81	3.15	2.16	0.39	2.55	1.59	0.14	1.73	1.26	0.08	1.34	1.21	0.07	1.28
Fugitt[23]	$T_t \leq 55$ $T_t > 55$	3.1×10^{98} 5.0×10^{45}	150,000 70,800	0.18	0.09	0.27	0.28	0.08	0.36	0.45	0.07	0.52	0.74	0.06	0.80	1.21	0.07	1.28
[illegible][24]	$T_t \leq 53$ $T_t > 53$	3.1×10^{98} 3.1×10^{98}	150,000 $150{,}000-122(T_t-53)$	0.66	0.24	0.90	0.78	0.17	0.95	0.84	0.09	0.93	0.87	0.06	0.93	0.95	0.06	1.01
Weaver & Stoll[6]	$T_t \leq 50$ $T_t > 50$	2.185×10^{124} 1.823×10^{51}	187,070 78,220	0.94	0.42	1.36	1.37	0.35	1.72	1.95	0.29	2.24	2.50	0.27	2.77	3.03	0.27	3.30
Takata[7]	$T_t \leq 50$ $T_t > 50$	4.322×10^{64} 9.389×10^{104}	100,000 160,000	2.15	0.72	2.87	1.85	0.32	2.17	1.24	0.10	1.34	0.91	0.06	0.97	0.86	0.04	0.90

NBS-114A (REV. 2-8C)

U.S. DEPT. OF COMM. BIBLIOGRAPHIC DATA SHEET (See instructions)	1. PUBLICATION OR REPORT NO. NBSIR 81-2320	2. Performing Organ. Report No.	3. Publication Date July 1981

4. TITLE AND SUBTITLE

A Heat Transfer Analysis of Scald Injury

5. AUTHOR(S)

Robert L. Palla, Jr.

6. PERFORMING ORGANIZATION (If joint or other than NBS, see instructions)

NATIONAL BUREAU OF STANDARDS
DEPARTMENT OF COMMERCE
WASHINGTON, D.C. 20234

7. Contract/Grant No.

8. Type of Report & Period Covered

9. SPONSORING ORGANIZATION NAME AND COMPLETE ADDRESS (Street, City, State, ZIP)

10. SUPPLEMENTARY NOTES

☐ Document describes a computer program; SF-185, FIPS Software Summary, is attached.

11. ABSTRACT (A 200-word or less factual summary of most significant information. If document includes a significant bibliography or literature survey, mention it here)

Numerical solutions for skin tissue temperature during scald injury events are obtained and utilized in conjunction with a thermal injury criterion, to predict critical exposure levels for various heated fluids. A one-dimensional tissue model of the type used by Love is employed to determine the initial tissue temperature distribution. The bio-heat equation for tissue heat transfer is then solved via an implicit finite difference technique, subject to convective heating and cooling at the surface.

The sensitivity of the critical exposure level to variations in tissue properties and convective heating coefficients is investigated. Thermal injury thresholds are presented for various fluids along with bounds to reflect uncertainty in assumed tissue properties. The results obtained are in good agreement with existing experimental scald injury data.

12. KEY WORDS (Six to twelve entries; alphabetical order; capitalize only proper names; and separate key words by semicolons)

Bioheat equation; burn; criterion; critical exposure; fluid; heat transfer; injury threshold; scald; thermal injury

13. AVAILABILITY

☒ Unlimited

☐ For Official Distribution. Do Not Release to NTIS

☐ Order From Superintendent of Documents, U.S. Government Printing Office, Washington, D.C. 20402.

☐ Order From National Technical Information Service (NTIS), Springfield, VA. 22161

14. NO. OF PRINTED PAGES 65

15. Price $8.00